# A Gas-Expanded Liquid Nanoparticle Deposition and Supercritical Drying Process to Reduce Adhesion of Microstructures

Kendall M. Hurst, W. Robert Ashurst, Christopher B. Roberts*
Department of Chemical Engineering, 212 Ross Hall, Auburn University, AL USA 36849
croberts@eng.auburn.edu, phone: 1-334-844-4827, fax: 1-334-844-2063

## ABSTRACT
It is well established that supercritical fluids such as supercritical $CO_2$ are dense fluids that do not demonstrate the often detrimental surface tensions and interfacial phenomena exhibited by other liquids. Supercritical $CO_2$ has hence become widely used in the microelectromechanical systems (MEMS) industry to dry release devices while avoiding the liquid-vapor interface that can cause the capillary collapse of microstructures. Unfortunately, due to the extremely high surface-area-to-volume ratio and the relative smoothness of such microstructures, strong adhesion still occurs during the operation of supercritically dried devices, yielding very short lifetimes. Our previous work has shown that ligand-stabilized gold nanoparticles can be precipitated from solution and deposited into wide-area films using $CO_2$- or gas-expanded liquids (GXLs). Following the liquid expansion and particle deposition, the nanoparticle films are dried by transitioning the $CO_2$-organic solvent mixture into the supercritical region. In this work, polysilicon cantilever beams are coated with gold nanoparticles via a GXL induced deposition process to increase the surface roughness of the relatively smooth microstructures, and then dried with supercritical $CO_2$. The GXL deposition/supercritical drying process was shown to have no detrimental effects on the polysilicon microstructures and the structures exhibited a drastic decrease in adhesion surface energy when nanoparticles were present. The intentional deposition of particulates onto MEMS and microstructures via GXLs/supercritical drying is a fundamentally new concept which shows promise in being adapted for commercial and industrial MEMS processes.

## INTRODUCTION
Microelectromechanical systems (MEMS) are miniature devices that directly couple micro-scale mechanical and electrical components into very small packages. MEMS are currently used industrially and commercially for applications such as accelerometers [1], ultra-miniature pressure sensors [2] and, more recently, digital micro-mirror devices (DMDs) [3]. Based on the initial success of current applications, MEMS are poised to have a major impact on industry and consumer products. The key benefits of MEMS result from inherent performance enhancements and reductions in manufacturing costs due to their miniature size [4]. However, the miniaturization of MEMS and microdevices also brings forth inherent reliability concerns which can affect the operational lifetime of the device. Typically, micromachined MEMS include a number of surface microstructures with lateral dimensions of 50-500 μm and thicknesses of 0.1-10 μm which are generally raised only 0.1-5 μm from the substrate surface. Due to the extremely large surface-area-to-volume ratio of such structures and components, surface and interfacial forces play an increased role in the operation of MEMS [5-8]. These interfacial and surfaces forces can cause device failure by promoting unwanted adhesion and wear.

One of the major bottlenecks preventing the commercialization of more complex MEMS-based products is that of stiction, or unwanted adhesion, which occurs between two contacting surfaces [5-10]. This adhesion results when the mechanical restoration forces of the structures are unable to overcome the interfacial forces (capillary, van der Waals,

electrostatic, chemical) holding them in place [4, 10-11]. Commonly, two types of stiction between micromachined structures can occur: release stiction and in-use stiction. Release stiction occurs following the microfabrication process when sacrificial layers are etched and MEMS components are dried. The liquid-vapor interface created by an evaporating liquid during drying yields tremendous capillary forces which draw surfaces into contact and render them permanently adhered [12-13]. Release stiction is most often avoided by the use of special drying techniques that eliminate the liquid-vapor interface, including critical point (or supercritical $CO_2$) drying [14-15]. In-use stiction, on the other hand, can occur at any time during the operation of a device when contacting microstructures experience attractive surface forces that exceed the mechanical restoration forces of the structures [7]. Several groups have performed ongoing research to reduce or eliminate the causes of in-use stiction.

Early attempts to reduce operational adhesion focused primarily on the reduction of the real contact surface area between two structures by increasing the surface roughness of the silicon-based materials [16-17]. These initial attempts, however, achieved only moderately improved results. Therefore, more recent efforts have focused on chemically altering the surfaces, typically by means of self-assembled monolayers (SAMs) [11]. SAM coatings on MEMS and microstructures have been demonstrated to effectively reduce adhesion, measured as the apparent work of adhesion, by up to four orders of magnitude [6, 18-19]. Unfortunately, SAM formation processes via organic molecular precursors are limited by their reaction sensitivity and reproducibility. Consequently, polysilicon surface roughening modifications were revisited by DelRio et al. [4] by studying the effect of 20-50 nm silicon carbide (SiC) particles on interfacial adhesion. Their results indicated that nanoparticulates can strongly influence the adhesion of microstructures by increasing the average separation distance between contacting surfaces. However, the SiC particles examined by DelRio et al. were inadvertently deposited onto the silicon surfaces as a reaction by-product during fabrication of microstructures. Previously, there have been no well established methods for depositing nanoparticles onto MEMS and microstructured devices. This is because solutions of nanoparticles cannot be drop cast onto microstructure surfaces by solvent evaporation due to the dewetting capillary effects that would result from the liquid-vapor interface. Drop casting of particles onto these surfaces would cause deformation and lead to device failure. The goal of this work, therefore, was to engineer a particle deposition process that is compatible with current MEMS fabrication methods to provide anti-adhesive properties.

Roberts et al. have previously demonstrated the precipitation of dispersed nanoparticles into uniform, wide area thin films using gas-expanded liquids (GXLs) [20-22]. During this process, $CO_2$ is added to an organic nanoparticle dispersion, effectively reducing the solvent strength and promoting nanoparticle precipitation. Following precipitation, the $CO_2$/organic solvent mixture is elevated to the supercritical regime which eliminates the liquid-vapor interface. Isothermal depressurization from the supercritical state then allows for the drying of nanoparticle-coated samples while avoiding the liquid-vapor interface and the associated detrimental dewetting effects. This paper investigates the use of GXLs to deposit nanoparticles onto polysilicon microstructures and the impact of these nanoparticles on adhesion.

## MATERIALS AND METHODS

Dodecanethiol-capped gold nanoparticles were synthesized by a two-phase liquid arrested precipitation process similar to that of Sigman et al. [23]. All chemical used were purchased from Alfa Aesar (Ward Hill, MA, USA). First, 36 mL of 26.8 mM aqueous solution of hydrogen tetrachloroaurate was combined with 2.7 g of the phase transfer catalyst tetraoctylammonium bromide in 24.5 mL toluene. After stirring the mixture for 1 h, the aqueous phase was removed and discarded, leaving a yellow organic phase containing gold

ions. This organic portion was then combined with 30 mL of 440 mM aqueous sodium borohydride solution, reducing the ions to the ground metallic state. The mixture was stirred vigorously for 8-10 h to allow for particle growth before removing and discarding the clear, aqueous phase. 240 μL of 1-dodecanethiol was then added to the deep red organic phase and stirred for 4 h to cap and stabilize the gold nanoparticles. The particle dispersion was then centrifuged with equal parts ethanol at 4500 rpm for 5 min to rinse the particles and remove excess thiol and reducing agent molecules. After several rinses, the particles were dispersed and stored in hexane. By transmission electron microscopy (TEM), the average diameter of the spherical gold nanoparticles was determined to be 5.0±1.2 nm.

GXL particle deposition was performed within a 30 mL stainless steel high pressure vessel, equipped with temperature control and a pressure transducer, connected to two 500-mL ISCO piston pumps (Teledyne ISCO, Lincoln, NE, USA) as illustrated in Figure 1. A sample desired to be coated with nanoparticles was first carefully transferred from within a hexane-filled storage vial into a 10 mm deep, ~14.25 mm diameter open-ended glass vial partially filled with hexane. Approximately 25 μL of concentrated gold nanoparticle dispersion (in hexane), average particle diameter of about 5 nm, was then added to the vial and carefully mixed. This open-ended glass vial was then sealed within the high pressure vessel using Teflon o-rings.

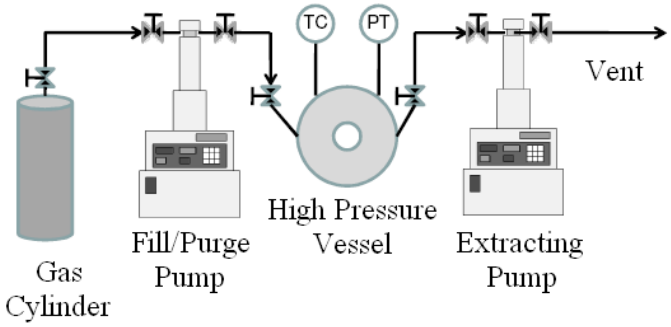


**Figure 1 : Illustration of the GXL particle deposition experimental setup.**

Once sealed, the vessel was pressurized with $CO_2$ to ca. 23 bar at room temperature (ca. 22 °C) using one of the 500-mL piston pumps. The vessel was then further pressurized, by setting the pump flow rate between 0.2 and 0.6 mL/min, to just beyond the vapor pressure of $CO_2$ (ca. 58 bar at 22 °C). During this pressurization, gold nanoparticles, within the open-ended glass vial, were allowed to precipitate out of solution and deposit onto the sample surface. Following precipitation, the $CO_2$/hexane mixture was heated isochorically to 40 °C to achieve a supercritical state. The vessel was then flushed with several volumes of pure supercritical $CO_2$ (at 40 °C and ca. 90 bar) at a rate of approximately 0.5 mL/min to ensure the removal of hexane from the vessel. Finally, the vessel was slowly depressurized at 40 °C by venting through a water-filled Schlenk tube to the atmosphere. The dry, gold nanoparticle-coated sample was then removed from the vessel for analysis. A more detailed account of the GXL particle deposition and supercritical drying process has been submitted for publication [24].

Test samples used to investigate the anti-adhesive properties of nanoparticle coatings consisted of polysilicon cantilever beam arrays (CBAs) provided by Sandia National Laboratories (Albuquerque, NM, USA). Each CBA consists of sixteen beams measuring 18 μm wide, 2.5 μm thick, and ranging between 150 to 1700 μm in length. The cantilever beams, anchored on only one end, are suspended approximately 2 μm from the underlying polysilicon substrate. To evaluate the effectiveness of nanoparticle films on adhesion, these polysilicon CBAs were coated with gold nanoparticles and analyzed via interferometry.

Native silicon oxide-coated and gold nanoparticle-coated CBAs were actuated by applying electrostatic loading using voltages from 0 V to 120 V in 10 V increments. The loading was then decreased in 10 V decrements to return to an unloaded state (0 V), concluding one actuation cycle. Adhesion of individual cantilever beams was then quantified using interferometrically collected experimental data to determine the apparent work of adhesion following a method similar to Mastrangelo [6].

**RESULTS**

Scanning electron microscopy (SEM) and atomic force microscopy (AFM) were used to characterize the deposition of 5-nm diameter gold nanoparticles on polysilicon CBAs and Si(100) monocrystalline surfaces. Figure 2 presents SEM images of (a) native oxide-coated and (b) gold nanoparticle-coated cantilever beams. The images illustrate that the nanoparticles deposited via the GXL process conformally coat every surface of the polysilicon beams and substrate. Figure 2b, however, indicates that the deposited particulates are more on the order of 10-20 nm in size; larger than the 5-nm diameter of the particles used for the coating. The joining of these particles to form islands is reminiscent of Volmer-Weber film growth [25]. This island formation is advantageous because it further increases the surface roughness of the microstructures, therefore further reducing the real contact surface area between two contacting surfaces. The root-mean-square (rms) roughness, determined by AFM, of a very clean Si(100) surface is typically around 0.2 nm. The rms roughness of a Si(100) surface coated with gold nanoparticle islands, however, is approximately 6 nm. This signifies that the deposited gold nanoparticles do in fact increase the surface roughness of the silicon surface.

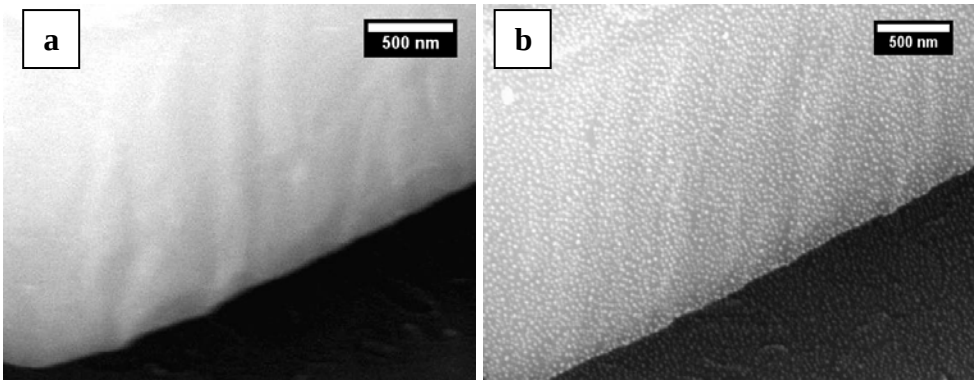


**Figure 2 : SEM images of (a) native oxide-coated and (b) gold nanoparticle coated cantilever beams. Darker surface is the substrate 2 μm below the beam.**

Cantilever beams coated with native oxide layers and gold nanoparticle coatings were electrostatically actuated, as discussed in the preceding section, in order to determine the effect of nanoparticle coatings on microstructure adhesion. Figure 3 presents two top-view interferograms of a native oxide-coated array of cantilever beams (a) before and (b) after one actuation cycle. Figure 3a represents initially free standing, unloaded beams as indicated by a lack of interference fringes. Following one actuation cycle, as described previously, every beam within the array was permanently adhered to the substrate, as illustrated by the interference fringes shown in Figure 3b. The in-sets in Figure 3 present a "side-view" of a selected beam before and after the actuation cycle, illustrating the adhesion of the beam. To quantify the adhesion of the beams shown in Figure 3b, the apparent work of adhesion was determined. The average apparent work of adhesion for the CBA in Figure 3b was 700±100 $\mu J/m^2$, which was great enough to permanently adhere every beam of the array.

By contrast, CBAs coated with 5-nm gold nanoparticles were also analyzed following the same actuation cycle as the native oxide-coated beams. Figure 4 presents interferograms of one gold nanoparticle-coated CBA (a) before and (b) after the actuation cycle. Once again, the lack of interference fringes in Figure 4a illustrates the free-standing nature of the cantilever beams prior to actuation. This image confirms that gold nanoparticles can be deposited onto microdevices via GXL deposition and supercritical drying without detrimentally affecting the microstructures. Following the actuation, some of the beams in the particular array were released and returned to the original free-standing position, as shown in Figure 4b. In fact, all beams with lengths of 500 μm or less did not adhere to the substrate, while a portion of beams with lengths longer than 500 μm were permanently adhered. Using the shortest adhered beam (550 μm long), an upper-bound limit on the apparent work of adhesion was determined to be about 8 $\mu J/m^2$. This estimate on the work of adhesion is a great improvement over native oxide-coated microstructures as well as previous attempts to reduce microstructure adhesion. Several CBAs coated with gold nanoparticles were examined, all exhibiting the same reduction of adhesion.

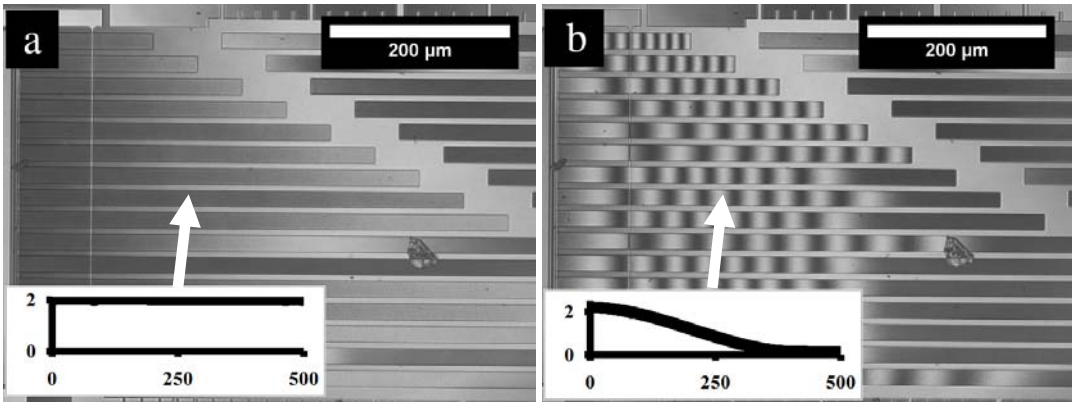


**Figure 3 : Interferograms of native oxide-coated CBA (a) before and (b) after one actuation cycle. Units of in-set are microns and not to scale with image.**

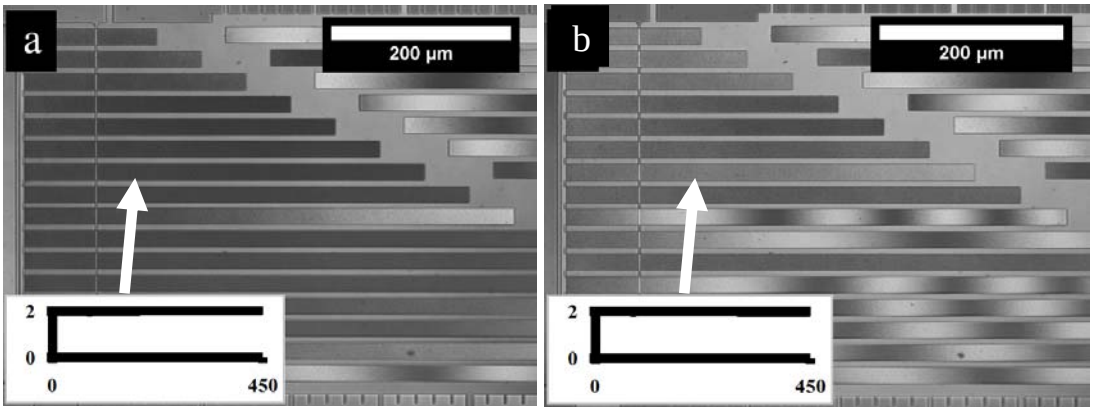


**Figure 4 : Interferograms of gold nanoparticle-coated CBA (a) before and (b) after one actuation cycle. Units of in-set are microns and not to scale with image.**

## CONCLUSION

In this study, gold nanoparticles were successfully deposited onto polysilicon microstructures by GXL deposition and supercritical drying. This GXL particle deposition technique is conformal and compatible with current MEMS microfabrication techniques as opposed to drop casting nanoparticles by solvent evaporation. In industry, this GXL deposition process may simply be introduced prior to the critical point (supercritical) drying step typically

performed following microfabrication. The nanoparticle coatings deposited in this study resulted in reduced microstructure adhesion by approximately two orders of magnitude compared to native silicon oxide-coated structures. These results suggest that the gold nanoparticles coatings reduce the inherent attractive surface forces, allowing the mechanical restoration forces of contacting microstructures to overcome the attraction that would cause permanent adhesion.

**REFERENCES :**


[1] CHAU, K. H. L., SULOUFF, R. E., Microelectronics Journal, Vol. 29, **1998**, p. 579.
[2] BURNS, D. W., ZOOK, J. D., HORNING, R. D., HERB, W. R., GUCKEL, H., Sensors and Actuators A, Vol. 48, **1995**, p. 179.
[3] VAN KESSEL, P. F., HORNBECK, L. J., MEIER, R.E., DOUGLASS, M. R., Proc. IEEE, Vol. 86, **1998**, p. 1687.
[4] DELRIO, F. W., DUNN, M. L., BOYCE, B. L., CORWIN, A. D., DE BOER, M. P., Journal of Applied Physics, Vol. 99, **2006**, p. 104304-1.
[5] RYMUZA, Z., Microsystem Technologies, Vol. 5, **1999**, p. 173.
[6] MASTRANGELO, C. H., Tribology Letters, Vol. 3, **1997**, p. 223.
[7] TAS, N., SONNENBERG, T., JANSEN, H., LEGTENBERG, R., ELWENSPOEK, M., Journal of Micromachines and Microengineering, Vol. 6, **1996**, p. 385.
[8] KOMVOPOULOS, K., Wear, Vol. 200, **1996**, p. 305.
[9] MABOUDIAN, R., Surface Science Reports, Vol. 30, **1998**, p. 207.
[10] MABOUDIAN, R., HOWE, R. T., Journal of Vacuum Science and Technology B, Vol. 15, **1997**, p. 1.
[11] MABOUDIAN, R., CARRARO, C., Annual Review of Physical Chemistry, Vol. 55, **2004**, p. 35.
[12] GUCKEL H., SNIEGOWSKI, J. J., CHRISTENSON, T. R., MOHNEY, S., KELLY, T. F., Sensors and Actuators A, Vol. 20, **1989**, p. 117.
[13] MASTRANGELO, C. H., HSU, C. H., Journal of Microelectromechanical Systems, Vol. 2, **1993**, p. 44.
[14] MULHERN, G. T., SOANE, D. S., HOWE, R. T., Transducers ’93, **1993**, p. 296.
[15] RESNICK, P. J., CLEWS, P. J., SPIE International Society for Optical Engineering, Vol. 4558, **2001**, p. 189.
[16] FAN, L. S., TAI, Y. C., MULLER R. S., Sensors and Actuators A, Vol. 20, **1989**, p. 41.
[17] YEE, Y., CHUN, K., LEE, J. D., KIM, C. J., Sensors and Actuators A, Vol. 52, **1996**, p. 145.
[18] MABOUDIAN, R., ASHURST, W. R., CARRARO, C., Sensors and Actuators A, Vol. 82, **2000**, p. 219.
[19] ASHURST, W. R., YAU, C., CARRARO, C., MABOUDIAN, R., DUGGER, M. T., Journal of Microelectromechanical Systems, Vol. 9, **2001**, p. 41.
[20] MCLEOD, M. C., KITCHENS, C. L., ROBERTS, C. B., Langmuir, Vol. 21, **2005**, p. 2414.
[21] MCLEOD, M. C., ANAND, M., KITCHENS, C. L., ROBERTS, C. B., Nano Letters, Vol. 5, **2005**, p. 461.
[22] LIU, J., ANAND, M., ROBERTS, C. B., Langmuir, Vol. 22, **2006**, p. 2964.
[23] SIGMAN, M. B., SAUNDERS, A. E., KORGEL, B. A., Langmuir, Vol. 20, **2005**, p. 978.
[24] HURST, K. M., ROBERTS, C. B., ASHURST, W. R., Nanotechnology, submitted for publication Dec 2008.
[25] OHRING, M., Materials Science of Thin Films: Deposition & Structure, San Diego: Academic Press, **2002**.